

Cell Systems, Volume 11

Supplemental Information

SYLARAS: A Platform for the Statistical

Analysis and Visual Display of Systemic Immunoprofiling

Data and Its Application to Glioblastoma

Gregory J. Baker, Jeremy L. Muhlich, Sucheendra K. Palaniappan, Jodene K. Moore, Stephanie H. Davis, Sandro Santagata, and Peter K. Sorger

Content

Fig. S1. Experimental Optimization for 12-color Immunophenotyping of GBM-bearing Mice by Flow Cytometry, Related to Fig. 1.

Fig. S2. Optical Spillover Among an Optimized Panel of 12 Mouse Immunophenotyping Antibodies is Fully Abrogated by Spectral Deconvolution, Related to Fig. 1.

Fig. S3. Cell Viability and Sample Counts for the 240 Lymphoid Tissues Analyzed in this Study, Related to Fig. 1.

Fig. S4. Dashboards from a SYLARAS screen of the GL261 Glioma Model, Related to Fig. 2.

Fig. S5. Antigen Expression by Different Mouse Immune Cell Subsets Identified via Prior Knowledge and Unsupervised Clustering Algorithms, Related to Fig. 4.

Fig. S6. Validation of a 12-channel t-CyCIF Antibody Panel, Related to Fig. 7.

Fig. S7. Survey of Glioma-infiltrating Lymphocytes by 12-channel t-CyCIF, Related to Fig. 7.

Table S1. Excel Spreadsheet for Calculating Reagent Dilutions (e.g. Antibodies, FVD, Fc Block, Injectable Anesthesia), Related to Fig. 1.

Table S2. Experimental Details for Performing 12-channel t-CyCIF on Mouse Brain FFPE Tissue Sections using Immune Lineage Markers, Related to Fig. 7.

Supplemental Information for SYLARAS

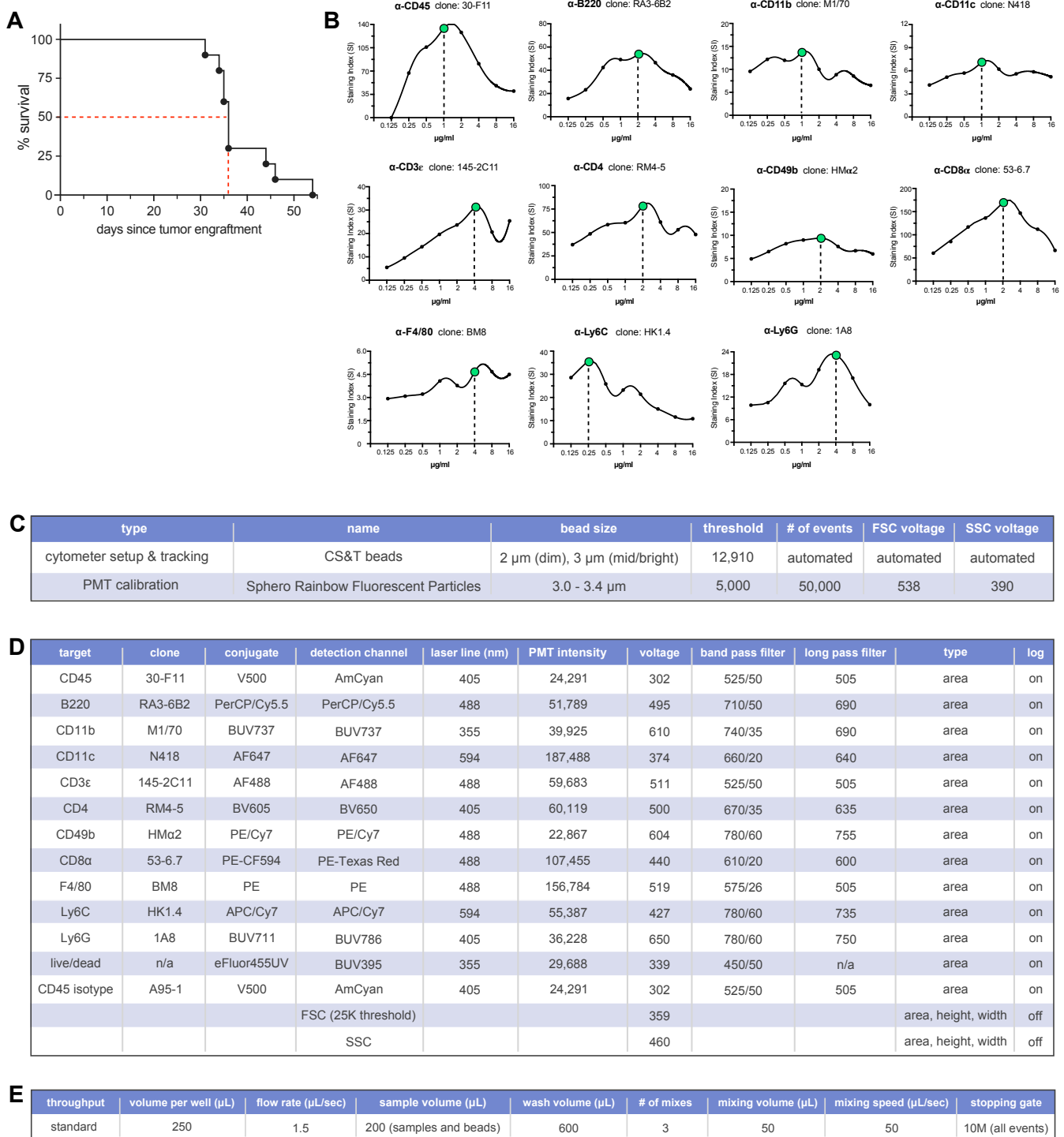


Fig. S1. Experimental Optimization for 12-color Immunophenotyping of GBM-bearing Mice by Flow Cytometry, Related to Fig. 1.

(A) Kaplan-Meier Survival Analysis of the GL261 Mouse Glioma Model. Ten (10) C57BL/6J mice were intracranially engrafted with 3×10^4 syngeneic GL261 cells at 12-weeks-of-age.

Fig. S1 (continued). Median survival (indicated by the intersecting dashed red lines) was 36-days post tumor engraftment. **(B)** 8-point, 2-fold serial dilution titration curves for 11 immune lineage markers using splenocytes from 12-week-old female C57BL/6J mice. Separation index (SI) was calculated as $(MFI_{\text{pos}} - MFI_{\text{neg}}) / [(84\%_{\text{neg}} - MFI_{\text{neg}}) / 0.995]$, where MFI_{pos} = median fluorescence intensity of the first positive peak, MFI_{neg} = median fluorescence intensity of the autofluorescence peak, $84\%_{\text{neg}}$ = 84th percentile of the autofluorescence peak (Telford et al., Cytometry A. 2009). Adjacent data points were interpolated with cubic splines. Antibody concentrations resulting in maximum SI values (SI_{max}) are indicated by green dots. Data acquisition gating strategy: (FSC-A vs. SSC-A) → (SSC-H vs. SSC-W) → (FSC-H vs. FSC-W) → (DAPI-A vs. FSC-A) → (CD_x vs. count). **(C)** Settings for cytometer setup/tracking and photomultiplier tube (PMT) calibration used to standardize cytometer performance across data acquisition cycles. **(D)** Cytometer run settings. **(E)** High-Throughput Sampler (HTS) configurations.

Supplemental Information for SYLARAS



Fig. S2. Optical Spillover Among an Optimized Panel of 12 Mouse Immunophenotyping Antibodies is Fully Abrogated by Spectral Deconvolution, Related to Fig. 1.

Signal intensity distributions of splenocytes from 12-week-old female C57BL/6J mice immunolabeled with an optimized 11-antibody immunomarker panel then stained with fixable viability dye (FVD).

Detection channels of a BD LSR II SORP flow cytometer (columns) are shown pre- and post-compensation. Antibodies (rows) are color-coded according to their target detection channel.

Histograms forming the downward diagonal from left to right across the matrix show the placement of the respective channel's compensation gate (blue-green interfaces).

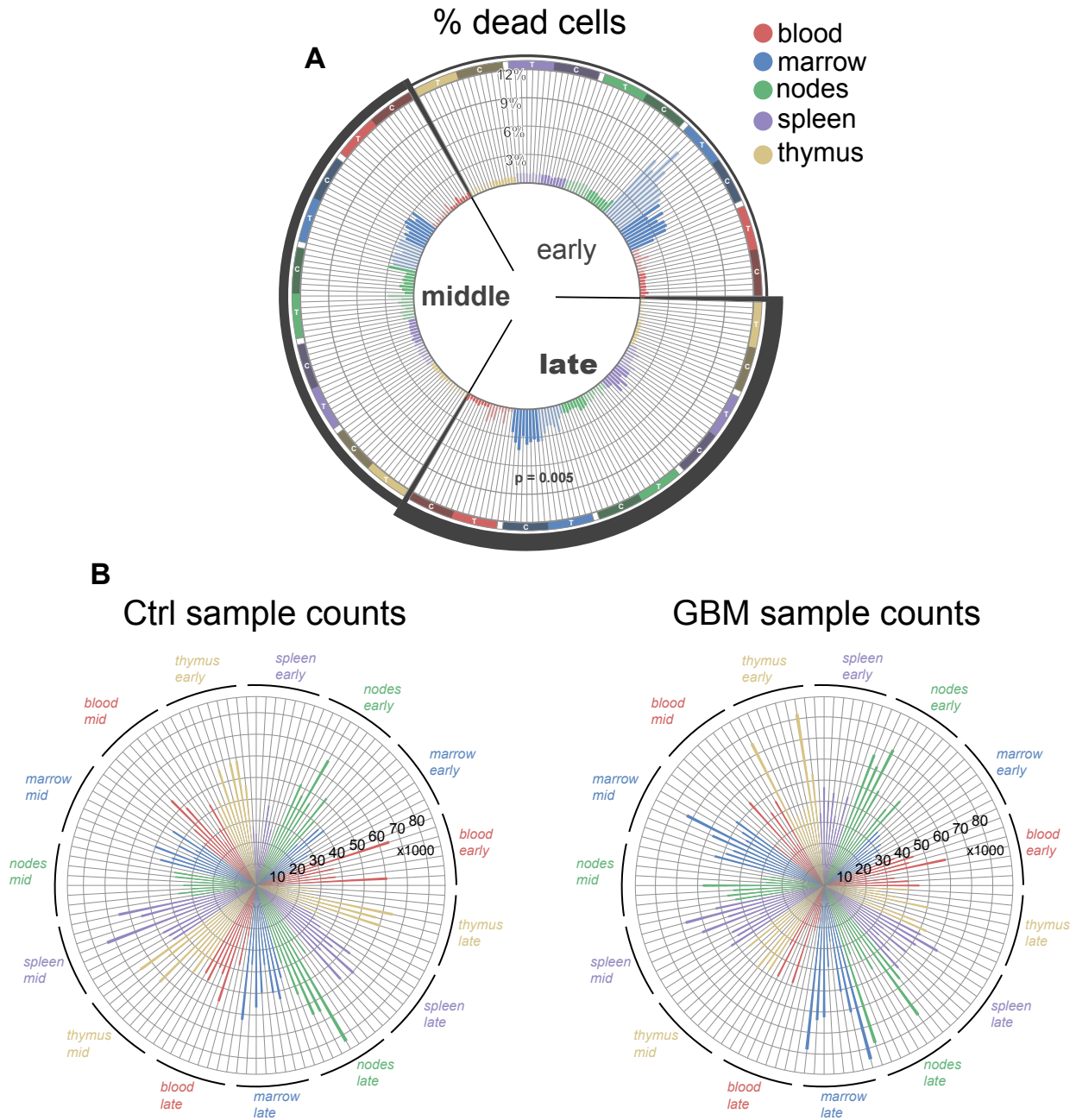
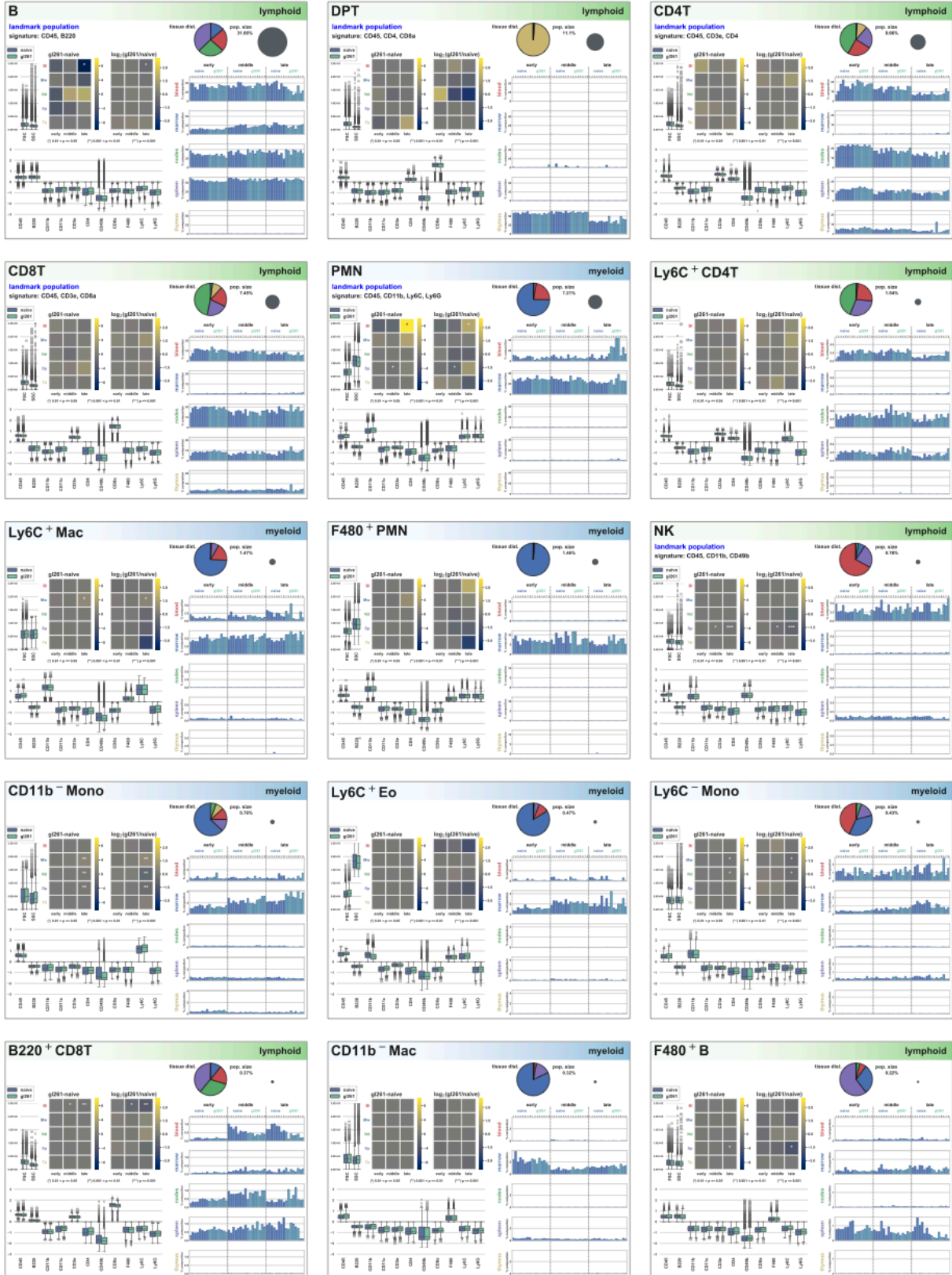


Fig. S3. Cell Viability and Sample Counts for the 240 Lymphoid Tissues Analyzed in this Study, Related to Fig. 1. (A) Radial bar chart showing the percentage of dead cells among the dataset's 240 tissue samples. C = control samples, T = GBM samples. Viability only differed between the two groups in the bone marrow at the t = 30-day time point ($p = 0.005$, two-tailed independent Student's t test, $n = 8$ mice/group). **(B)** Radial bar charts showing the number of cells in control (left) and GBM (right) mouse tissue samples after weighted random sampling by tissue to balance the number of cells per sample.



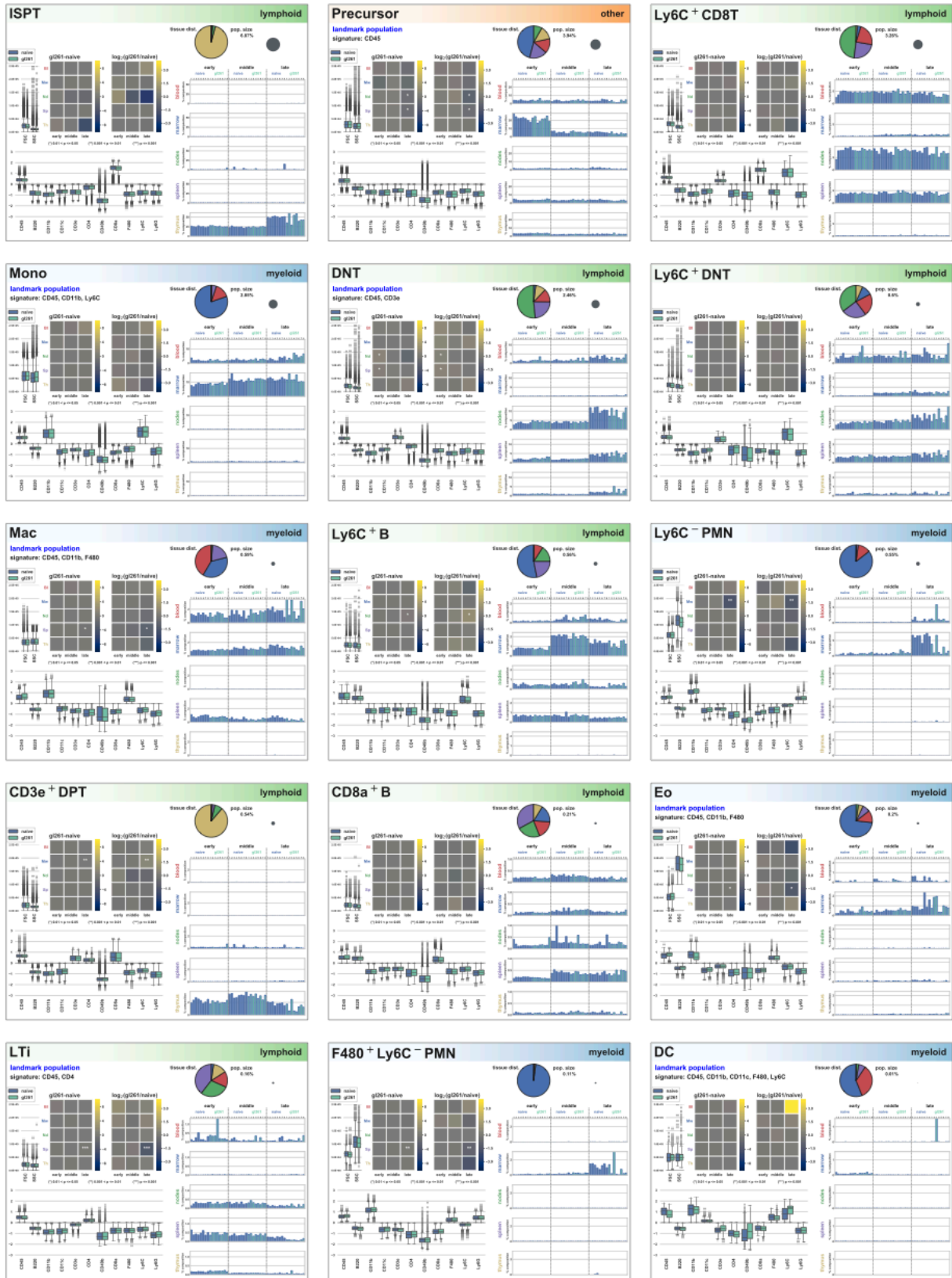
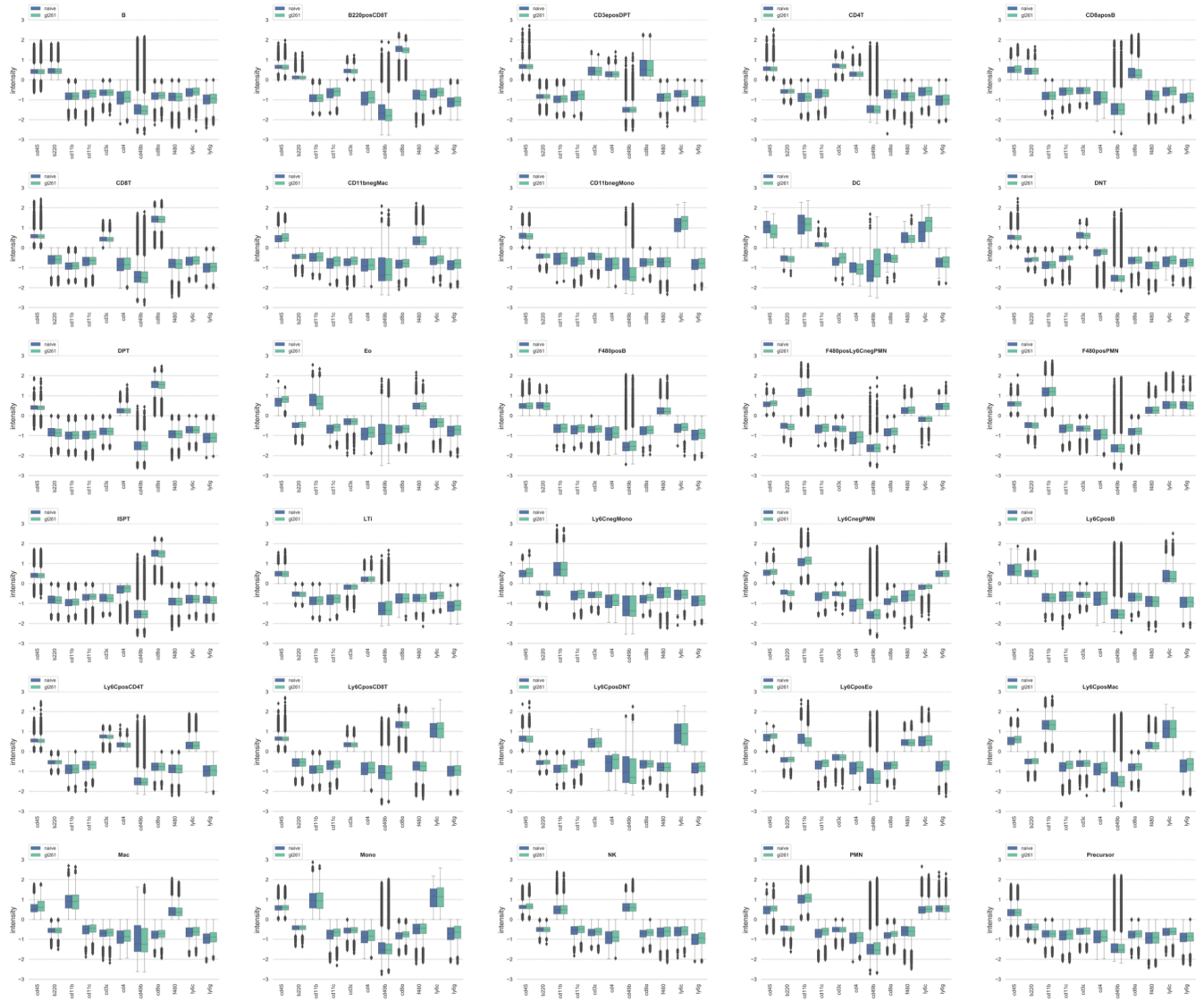


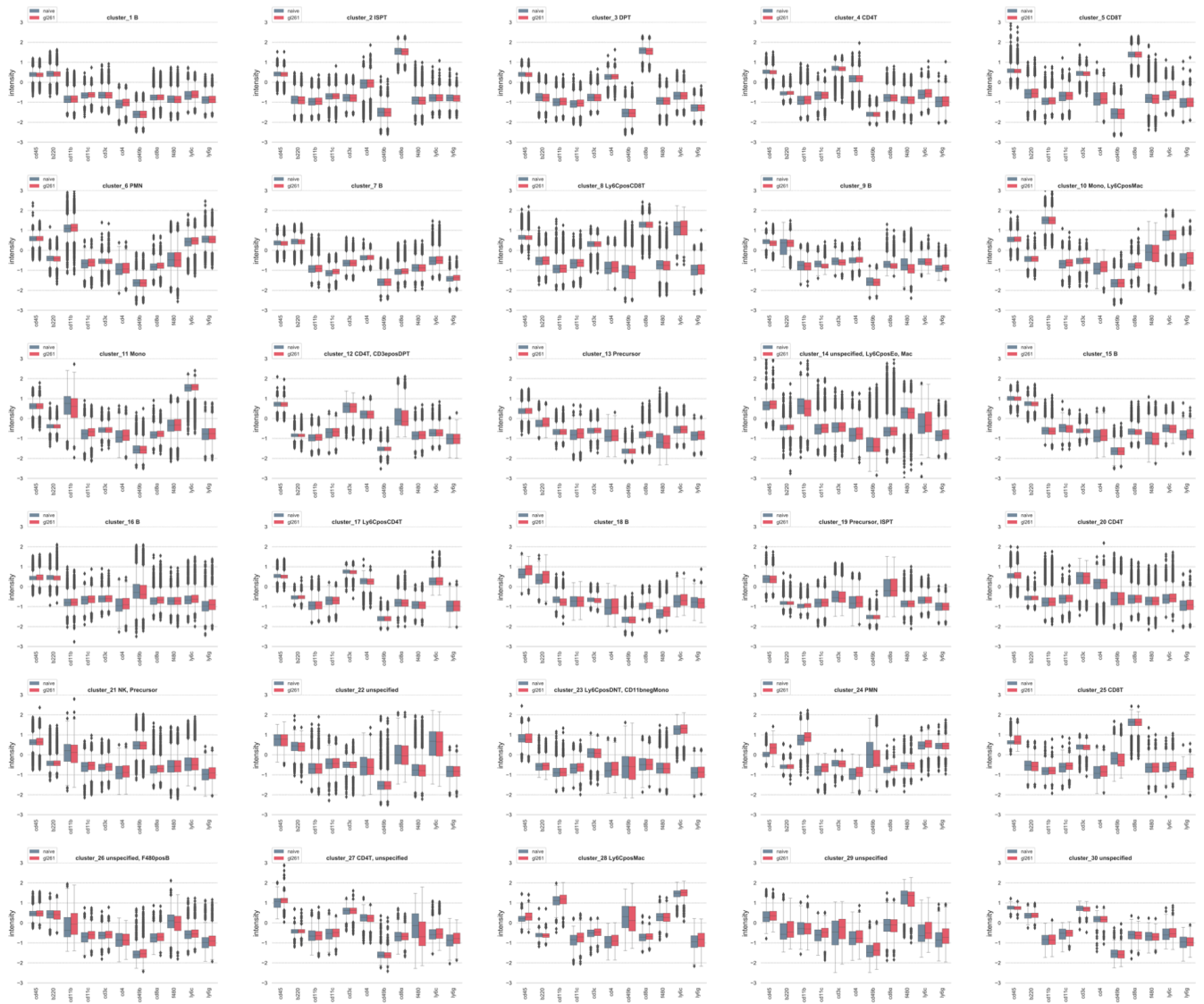
Fig. S4. Dashboards from a SYLARAS screen of the GL261 Glioma Model, Related to Fig. 2.

PDF available for download at: <https://www.synapse.org/#!Synapse:syn22249852>.

Manual Gating



PhenoGraph



FlowSOM

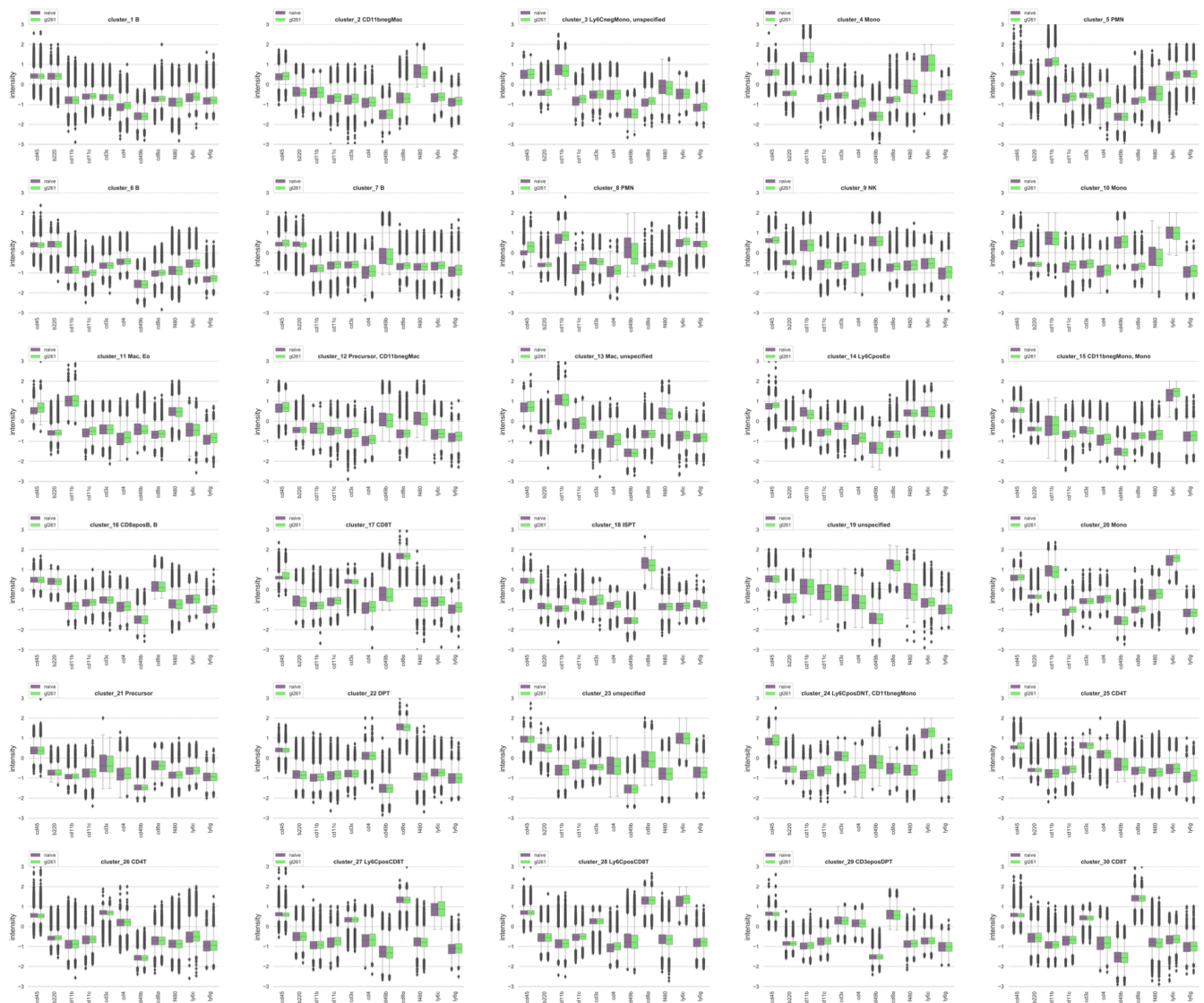
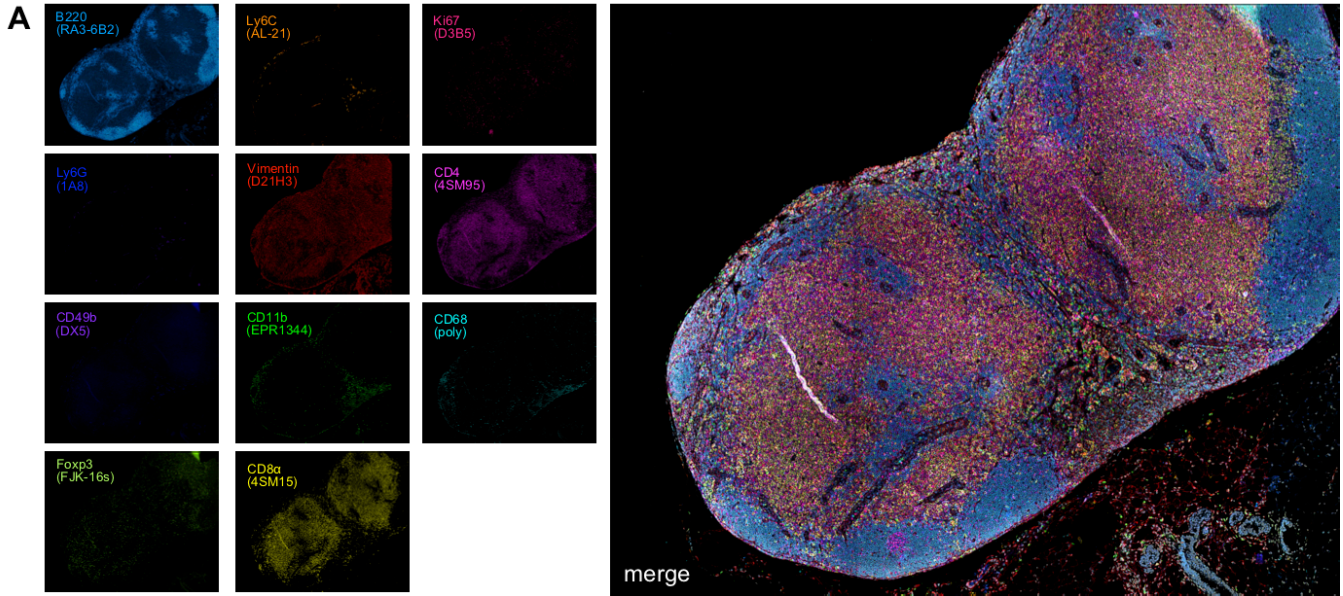


Fig. S5. Antigen Expression by Different Mouse Immune Cell Subsets Identified via Prior Knowledge and Unsupervised Clustering Algorithms, Related to Fig. 4.

Boxplot distributions of Logicle-transformed antigen expression by various immune cell subsets from control (naïve) and GBM-bearing (g1261) mice identified through manual gating (top), PhenoGraph clustering (middle), and FlowSOM clustering (bottom). PDF available for download at: <https://www.synapse.org/#!Synapse:syn22263977>.



See figure legend below for link to high-resolution TIFF.

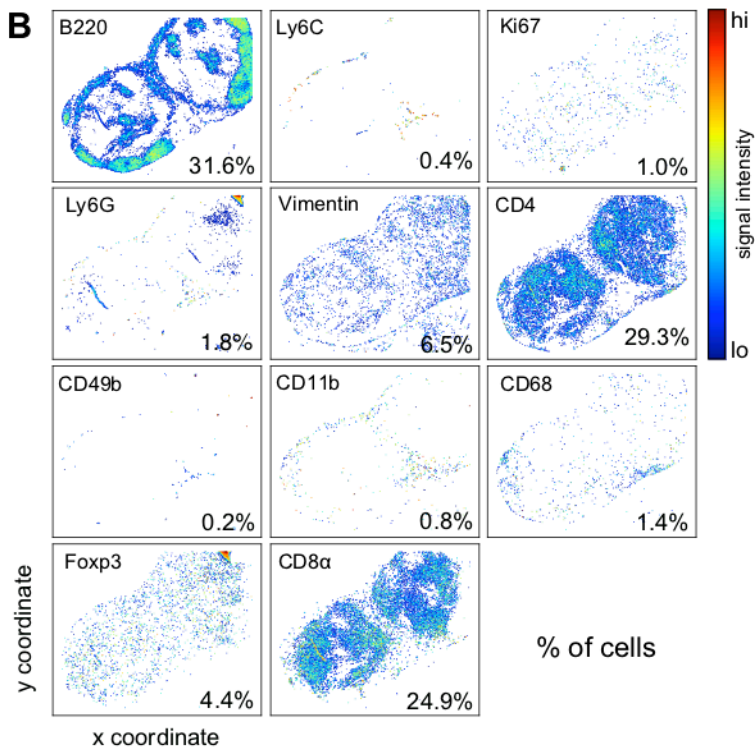
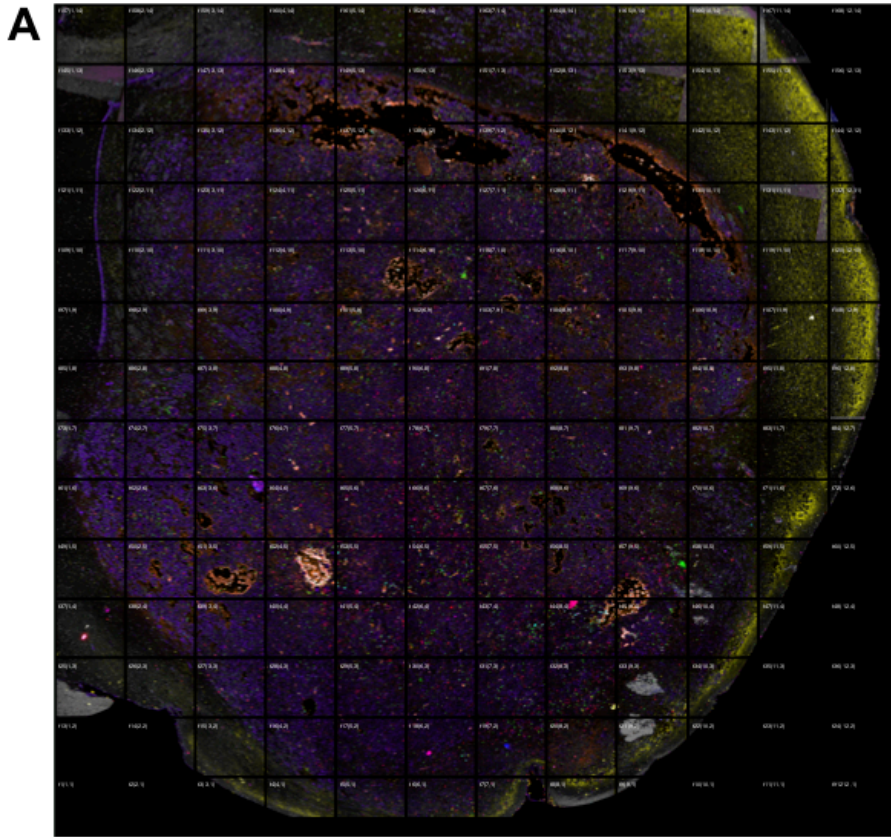


Fig. S6. Validation of a 12-channel t-CyCIF Antibody Panel, Related to Fig. 7.

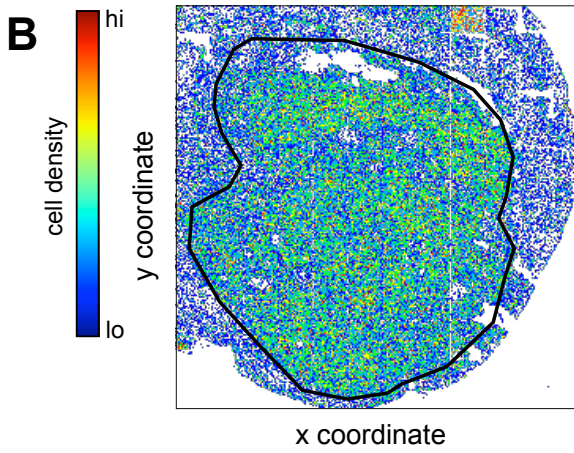
(A) 11 antibodies validated on inguinal lymph node FFPE tissue sections from a C57BL/6 mouse; individual channels (left) and composite image (right) are shown.

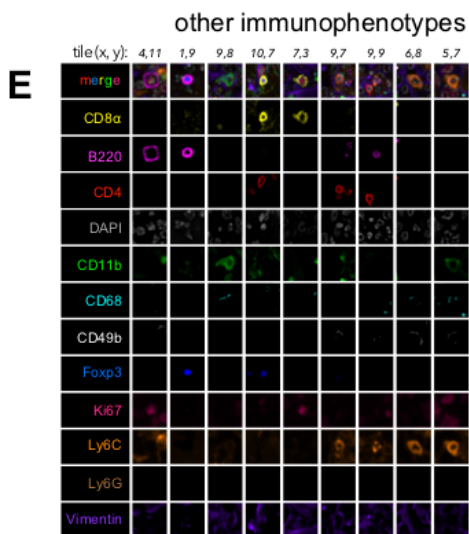
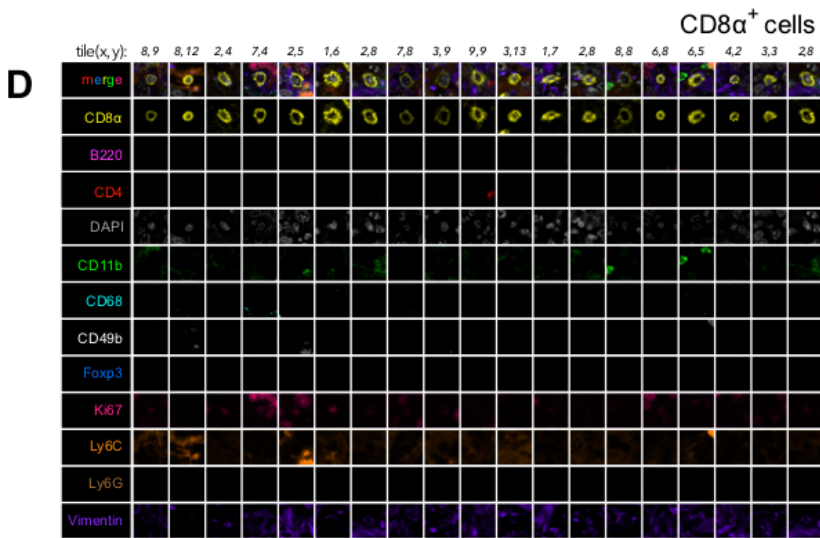
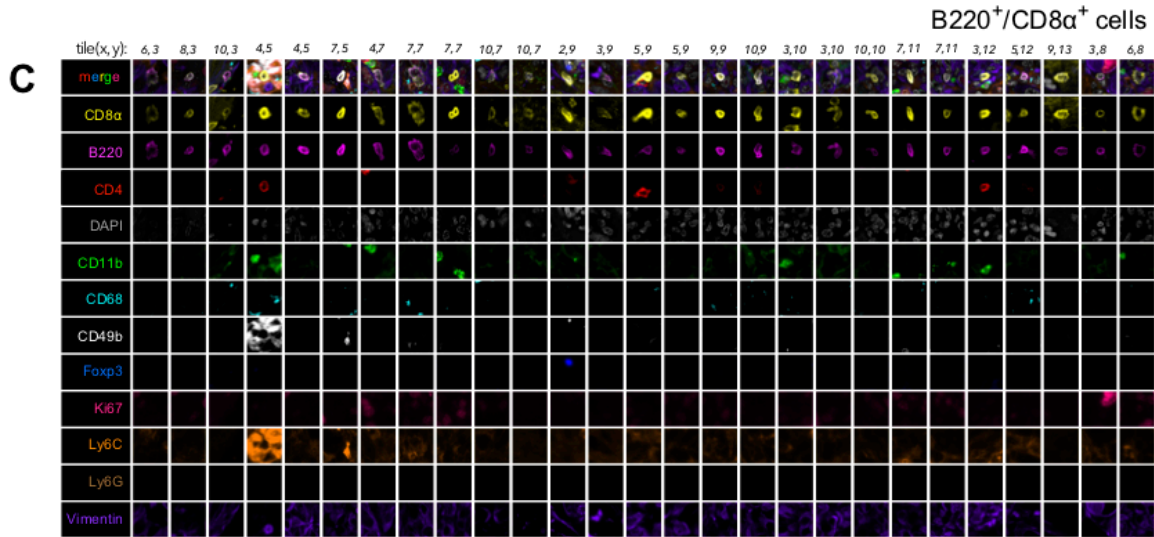
Fig. S6 (continued). High-resolution TIFF available for download at:

<https://www.synapse.org/#!Synapse:syn22249837>. **(B)** X and Y coordinates of cells from the micrograph shown in (A) color-coded according to antibody signal intensity; the percentage of total cells immunoreactive to each antibody is shown.



See figure legend below for link to high-resolution TIFF.





See figure legend below for link to high-resolution TIFFs.

Fig. S7. Survey of Glioma-infiltrating Lymphocytes by 12-channel t-CyCIF, Related to Fig. 7.

(A) A 12-channel (11 antibodies plus nuclear counter stain), 168-tile (400 μ m x 300 μ m fields of view) mosaic image taken at 40X of the tumor-ipsilateral mouse brain hemisphere bearing GL261 glioma 36-days after engraftment. Tile numbers and grid coordinates are indicated in increasing order from the bottom-left to the top-right of the image. Immunomarker colors are as in (C-E). High-resolution TIFF available for download at: <https://www.synapse.org/#!Synapse:syn22249837>. (B) X and Y coordinates of $\sim 9 \times 10^4$ cells extracted from the image shown in (A). Data points representing individual cells are colored according to cell density. Black perimeter outlines the tumor/brain parenchyma interface. (C) Examples of B220/CD8 α double-positive cells. Tile coordinates are provided for each image for cross-referencing with the image shown in (A). (D) Examples of CD8 α single-positive cells. Tile coordinates are provided for each image for cross-referencing with the image shown in (A). (E) Examples of other, lower abundance, immunophenotypes identified in the late-stage GL261 tumor microenvironment. Tile coordinates are provided for each image for cross-referencing with the image shown in (A). High-resolution TIFFs of (C-E) available for download at: <https://www.synapse.org/#!Synapse:syn22249837>.